Physicochem. Probl. Miner. Process., 62(6), 2026, 242673

http://www.journalssystem.com/ppmp

Physicochemical Problems of Mineral Processing

ISSN 1643-1049
© Wroclaw University of Science and Technology

Selective adsorption of different functional groups on kaolinite and coal surfaces: an MD and DFT study

Xuefeng Zhan [1], Chunyun Zhu [1,3], Fanfei Min [1,2], Lujun Wang [1], Hui Li [1]

[1] Department of Materials Science and Engineering, Anhui University of Science and Technology, Huainan 232001, Anhui, China

[2] School of Metallurgical Engineering, Anhui University of Technology, Ma'anshan 243000, Anhui, China

[3] State Key Laboratory for Safe Mining of Deep Coal Resources and Environment Protection, Anhui University of Science and Technology, Huainan 232001, China

Corresponding authors: aust_zcy@163.com (C Zhu), ffmin@aust.edu.cn (F Min)

Abstract: The selective flotation of kaolinite from high-ash fine coal slime offers a promising pathway to overcome the challenge of clay–coal separation. This study employed density functional theory (DFT) calculations, molecular dynamics (MD) simulations, and flotation experiments to compare the selective adsorption of different functional groups on kaolinite (001), (00-1), and coal surfaces, with the aim of identifying effective reagents for kaolinite flotation. DFT and MD results show that octylphosphonic acid exhibits the strongest interaction, lowest diffusion coefficient, smallest frontier orbital energy gap, and lowest adsorption energy on kaolinite (00-1), indicating selective recognition of the Al-OH surface. Octylamine adsorbs strongly on both kaolinite (001) and coal but weakly on kaolinite (00-1), whereas octanoic acid is intermediate. Flotation tests confirm these trends: octylphosphonic acid gives the highest kaolinite recovery (60.93%) and concentrate ash (78.37%) at 150 g/t while strongly suppressing combustible recovery, making it the most promising reagent for kaolinite flotation. Octylamine gives the highest combustible recovery (72.98%) at 450 g/t, whereas its lowest kaolinite recovery (25.93%) is observed at 600 g/t, indicating that it preferentially floats coal and is unsuitable for kaolinite flotation. Octanoic acid is intermediate. Overall, the phosphonic acid group is highly selective for the kaolinite Al-OH surface, the carboxyl group is moderate, and the amino group is unfavorable for kaolinite flotation. This study provides a fundamental theoretical basis for the design of selective flocculants in the coal-kaolinite separation system.

Keywords: kaolinite, coal, selective adsorption, molecular dynamics simulation, DFT

1. Introduction

As an inevitable byproduct (-0.5 mm) of coal development and utilization, fine coal slime is primarily upgraded via flotation (Yang et al., 2025). However, the flotation of high-ash coal slime faces persistent challenges, arising from the substantial specific surface area and complex surface characteristics of ultrafine clay particles. These factors collectively undermine separation efficiency and exacerbate both material waste and environmental concerns (Arcod et al., 2026; Niu et al., 2024). To address these challenges, selective flocculation has emerged as a promising strategy for fine mineral separation. In this process, polymeric flocculants preferentially bridge target mineral particles into settleable or floatable aggregates, thereby facilitating their separation from gangue minerals (Ng et al., 2026; Lu et al., 2026; Lv et al., 2026).

Selective flocculation performance is fundamentally governed by flocculant selectivity, and numerous flocculants have accordingly been investigated to address the challenge of separating coal fines from kaolinite and other clay gangues (Peng et al., 2024; Zhang et al., 2022; Zhang et al., 2026). In terms of modified natural polymers, Zhang et al. (2025) demonstrated that etherified starch enables selective flocculation of kaolinite, leading to improved coal quality and reduced ash content. Complementarily, Shi et al. (2026) combined experimental approaches with molecular dynamics

DOI: 10.37190/ppmp/242673

simulations to explore the adsorption mechanism of carboxymethyl guar gum on silica surfaces. In terms of synthetic polymers, research has mainly focused on functionalized polyacrylamide. For instance, Zou et al. (2019) introduced hydrophobic groups into the polyacrylamide chain, using it as a collector to improve the flotation recovery of fine coal. Meanwhile, Xia et al.[13] enhanced the selective flotation separation of fine non-coking coal from kaolinite by pretreating with anionic polyacrylamide. Furthermore, Ng et al. (2016) synthesized poly(N-isopropylacrylamide-co-ethyl xanthate methacrylate), a thermoresponsive polymer that functions dually as a flocculant and collector above its lower critical solution temperature (LCST). This dual functionality facilitated the selective flocculation and flotation of chalcopyrite from quartz sulfide fines. Their work thus provides a promising paradigm for the design of stimuli-responsive smart flocculants. However, most previous studies have focused primarily on macroscopic performance evaluation and polymer modification, while a systematic atomistic-scale understanding of the selective recognition and interaction mechanisms between typical functional groups (e.g., phosphonic acid, carboxyl, and amino groups) and coal/kaolinite surfaces remains scarce (Yuan et al., 2026; Xia et al., 2024; Huang et al., 2026). The complex conformations and multi-point adsorption effects of polymers may mask the selectivity of functional groups, making the molecular design of selective flocculants still rely, to some extent, on empirical screening (Zhang et al., 2022). Therefore, elucidating the inherent selectivity differences among functional groups is essential for transitioning flocculant design from an empirical to a more rational, mechanism-based approach.

Building on this, the present study systematically examines the differential interactions of three functional groups (phosphonic acid, carboxyl, and amino) with kaolinite versus coal surfaces, aiming to elucidate the microscopic mechanisms underlying selective adsorption. A combined approach of density functional theory (DFT) calculations, molecular dynamics (MD) simulations, and flotation experiments is employed to probe the adsorption behaviors from atomic to macroscopic scales. Through this multi-level analysis, this work seeks to establish a theoretical basis for the rational design of selective flocculants.

2. Experimental materials and methods

2.1. Materials

The bituminous coal sample used for micro-flotation experiments was collected from the Linhuan Coal Preparation Plant in the Huaibei mining area, China, and had an ash content of 8.82%. Kaolinite particles were supplied by Shanghai Macklin Biochemical Co., Ltd. (Shanghai, China). The octanoic acid (99%), octylamine (99%), octylphosphonic acid (95%), and 2-octanol (analytical grade) were also obtained from Macklin, and deionized water was used throughout all experiments.

2.2. DFT calculation

DFT calculations for adsorption on characteristic structural units of bituminous coal were performed using the CASTEP module in Materials Studio 2017 (Segall et al., 2002; Stewart et al., 2005), with initial adsorption-site screening conducted via Monte Carlo simulations in the Sorption module. Structure optimization in CASTEP was carried out using the BFGS algorithm, employing the GGA-PBE (Generalized Gradient Approximation-Perdew-Burke-Ernzerhof) exchange-correlation functional (Perdew et al., 1996) for electron exchange-correlation interactions, and incorporating the TS (Tkatchenko-Scheffler) correction (Khalil et al., 2020) to describe dispersion interactions. The Brillouin zone was sampled using only the Γ point. The self-consistent field (SCF) convergence tolerance was set to 2.0×10^{-6} eV/atom. A plane-wave cutoff energy of 400 eV was employed for the CASTEP calculations. No vacuum layer for periodic surface separation was introduced in the DFT models, as the DFT calculations did not employ a periodic slab model requiring such a vacuum region. Following structural optimization, the Locate task in the Sorption module was applied to precisely identify the adsorption sites. Energy optimization and property calculations were subsequently performed with the Dmol3 module, with all parameters set in accordance with established literature protocols (Chen et al., 2020).

The adsorption energy was calculated using the following formula:

$$E_{ads} = E_{total} - \left(E_{reagent} + E_{substrate}\right) \quad (1)$$

where E_{ads} is the adsorption energy， E_{total} is the total energy of the whole system, $E_{reagent}$ is the energy of the reagent molecule, and $E_{substrate}$ is the energy of the bituminous coal characteristic structural unit (or kaolinite surface). All these energies are in eV. A lower adsorption energy indicates more stable adsorption.

The adsorption geometries were optimized using the CASTEP module, and the corresponding adsorption energies were subsequently evaluated using the Dmol3 module based on the optimized structures. The calculated adsorption energies were primarily used to compare the relative adsorption tendencies of different reagent–substrate systems under a consistent computational protocol, rather than to determine highly accurate absolute binding energies. Therefore, the analysis mainly focuses on the relative variations and trends in adsorption energies.

The characteristic structural unit models of bituminous coal (Ph-OH, Ph-O-, Ph-C=O, Ph-COOH, Ph-CH_3) were constructed on the basis of the bituminous coal macromolecular model, with consideration of computational cost and capability, as shown in Fig. 1.

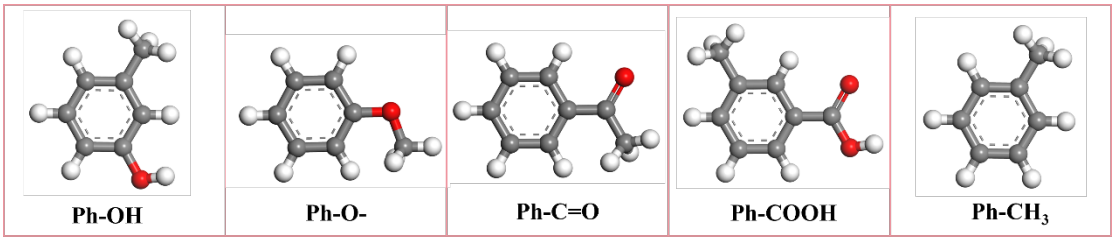
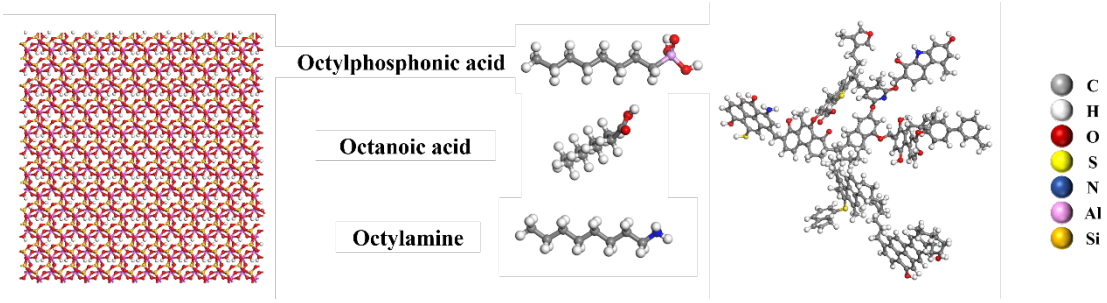


Fig. 1. Characteristic structural unit models of bituminous coal

2.3. MD simulation method

All model construction and calculations were performed using Materials Studio. Octylphosphonic acid, octanoic acid, and octylamine were selected as model compounds for phosphonic acid, carboxyl, and amino groups, respectively, with a C8 alkyl chain to confer moderate hydrophobicity while highlighting head-group effects. Initial molecular configurations were built and geometrically optimized (Fig. 2). The kaolinite unit cell, obtained from the American Mineralogist Crystal Structure Database, was expanded to a 10 × 6 × 1 supercell and cleaved to expose the (001) and (00-1) surfaces. The coal surface was constructed by repeatedly compressing the Wiser bituminous coal model (Cheng et al., 2023). Specifically, the Wiser coal model was placed between two graphene sheets separated by 15 Å, and the confined structure was subjected to geometry optimization. The resulting coal structure was then further optimized to obtain the coal model used in subsequent MD simulations. For each simulation box, five optimized molecules were placed on the bottom surface to attain approximately half-monolayer coverage on the kaolinite (001), (00-1), and coal surfaces, respectively. The Amorphous Cell module was then used to solvate the system with flexible SPC water molecules, and a vacuum layer of ~60 Å was added above the reagent/water layer to prevent spurious interactions between periodic images, yielding a final supercell of 51 Å × 53 Å × 145 Å. The PCFF force field was employed to describe the interactions among the coal surface, kaolinite surface, and reagent molecules. Atomic types and partial charges were assigned based on the corresponding PCFF force-field parameters implemented in Materials Studio. Water molecules were described using the flexible SPC model, with their partial charges and intramolecular parameters taken from the corresponding SPC parameter set. The selection of the PCFF/flexible-SPC combination was based on previous molecular dynamics studies, in which this combination had been applied to aqueous interfacial systems. The PCFF force field was employed under the NVT ensemble at 298 K, with three-dimensional periodic boundary conditions. The NVT ensemble was selected to maintain a constant number of particles, simulation-cell volume, and temperature throughout the simulations. This fixed-volume approach was appropriate for the present slab-based interfacial systems containing a substantial vacuum layer, as it maintained the prescribed cell dimensions and vacuum-layer thickness. In particular, pressure coupling could introduce undesirable changes in the simulation-cell dimensions in the presence of a large vacuum region. The Nosé thermostat was used to control the temperature at 298 K. Long-range electrostatic interactions were evaluated by the Ewald method, while van der Waals forces were computed with the Atom-based

method (Chen et al., 2022), using a cutoff radius of 25 Å. The MD simulation protocol consisted of three stages: energy minimization using the conjugate gradient algorithm, equilibration for 500 ps, and a subsequent production run of 200 ps. A time step of 1 fs was used throughout the equilibration and production stages. The 500 ps equilibration period allowed the initial interfacial configurations to relax, and trajectory monitoring indicated that the system had reached a stable state by the end of equilibration. The subsequent 200 ps production trajectory was used for property analysis, including interaction energies, self-diffusion coefficients derived from mean square displacement curves, and relative concentration distributions.



(a) Kaolinite cluster structure (b) Three molecular models (c) Bituminous coal model

Fig. 2. Kaolinite model, three molecular models, and bituminous coal model

2.4. Flotation method

Micro-flotation experiments were conducted using a 1:1 (by mass) mixture of kaolinite (-10 μm) and coal (-45 μm) at a solids concentration of 80 g/L in a 90 mL flotation cell. The initial pulp pH was recorded to range from 6 to 8. No deliberate pH adjustment was performed during the experiments. The pulp was first conditioned, followed by the addition of the target reagent and then 2-octanol as the frother. The conditioning time was 3 min, the flotation duration was 3 min, and the aeration rate was maintained at 0.2 m^3/h.

To evaluate the effect of the three reagents (octylphosphonic acid, octanoic acid, and octylamine) on kaolinite recovery, flotation tests were performed at dosages of 0, 150, 300, 450, and 600 g/t under optimized conditions. Flotation performance was assessed in terms of concentrate yield, concentrate ash content, combustible recovery, and kaolinite recovery. After flotation, the concentrate was filtered, dried, and weighed, and the concentrate yield was calculated by Equation (2):

$$\gamma = \frac{m}{M} \times 100\% \tag{2}$$

where γ is the concentrate yield (%), m is the mass of concentrate (g), and M is the mass of flotation feed (g).

The concentrate ash content was calculated by Equation (3):

$$A_d = \frac{m_1}{m} \times 100\% \tag{3}$$

where A_d is the concentrate ash content (%), and m_1 is the mass of ash in the concentrate (g).

Combustible recovery and kaolinite recovery were calculated by Equations (4) and (5), respectively:

$$\varepsilon = \frac{\gamma \cdot (100 - A_d)}{100 - A_0} \times 100\% \tag{4}$$

$$E = \gamma \frac{A_d - A_c}{A_0 - A_c} \tag{5}$$

where ε is the combustible recovery (%), A_c is the ash content of the raw coal (8.82%), A_0 is the measured ash content of the feed mixture (54.16%), and E is the kaolinite recovery (%).

3. Results and snalysis

3.1. DFT calculation results

3.1.1. Frontier orbital analysis

Frontier orbital theory states that a smaller energy gap (ΔE) between the highest occupied molecular orbital (HOMO) of one reactant and the lowest unoccupied molecular orbital (LUMO) of the other

facilitates more favorable intermolecular interactions (Liu et al., 2019).To further understand the adsorption active sites and reactivity between molecules, the frontier orbital energy differences between octylphosphonic acid, octanoic acid, octylamine and the bituminous coal characteristic structural units, kaolinite (001) face, and kaolinite (00-1) face were calculated according to Equations (6)–(11):

$$\Delta E_1 = \left|E^c_{HOMO} - E^l_{LUMO}\right| \quad (6)$$

$$\Delta E_2 = \left|E^c_{HOMO} - E^a_{LUMO}\right| \quad (7)$$

$$\Delta E_3 = \left|E^c_{HOMO} - E^s_{LUMO}\right| \quad (8)$$

$$\Delta E_4 = \left|E^l_{HOMO} - E^c_{LUMO}\right| \quad (9)$$

$$\Delta E_5 = \left|E^a_{HOMO} - E^c_{LUMO}\right| \quad (10)$$

$$\Delta E_6 = \left|E^s_{HOMO} - E^c_{LUMO}\right| \quad (11)$$

where E^c_{HOMO} and E^c_{LUMO} are the HOMO and LUMO energies of the kaolinite (001) face, kaolinite (00-1) face, and bituminous coal characteristic structural units, in eV. E^l_{HOMO} and E^l_{LUMO} are those of octylphosphonic acid. E^a_{HOMO} and E^a_{LUMO} are those of octylamine. E^s_{HOMO} and E^s_{LUMO} are those of octanoic acid.

Table 1 lists the HOMO-LUMO energy gaps (ΔE) for different reagent–surface combinations. The data indicate that ΔE_1 (octylphosphonic acid with coal/kaolinite) consistently exceeds ΔE_4 (octylphosphonic acid with kaolinite (00-1)). For Ph-C=O and Ph-COOH, ΔE_2 and ΔE_3 (involving octanoic acid and octylamine) are larger than ΔE_5 and ΔE_6 (involving their LUMO interactions), whereas the opposite trend holds for Ph-OH, Ph-O-, and Ph-CH_3. On the basis of frontier orbital theory, these results suggest three interaction patterns. Firstly, the HOMO of octylphosphonic acid preferentially interacts with the LUMO of kaolinite and coal structural units. Secondly, the HOMO of octanoic acid and octylamine is more reactive toward the LUMO of kaolinite, Ph-C=O, and Ph-COOH. Thirdly, the LUMO of octanoic acid and octylamine preferentially interacts with the HOMO of Ph-OH, Ph-O- and Ph-CH_3. Notably, the smallest ΔE_4 for the kaolinite (00-1) surface indicates the most stable adsorption of octylphosphonic acid on this surface, consistent with the MD and DFT results above. As shown in Fig. 3, the HOMO orbitals of the three reagents are mainly localized on their polar head groups. The HOMO orbitals of Ph-C=O and Ph-COOH are primarily distributed on the −C=O and −COOH groups, whereas those of Ph-OH, Ph-O-, and Ph-CH_3 are predominantly located on the benzene rings and oxygen-containing functional groups.

Table 1. Frontier orbital energies and energy differences of three reagents, kaolinite (001) face, kaolinite (00-1) face, and bituminous coal characteristic structural units

Group	Frontier orbital energy/eV		Frontier orbital energy difference/eV					
	E_{HOMO}	E_{LUMO}	ΔE_1	ΔE_2	ΔE_3	ΔE_4	ΔE_5	ΔE_6
Ph-C=O	-6.190	-2.865	7.607	6.773	5.975	3.382	4.319	4.362
Ph-COOH	-6.206	-2.347	7.623	6.789	5.991	3.900	4.837	4.880
Ph-OH	-5.190	-0.879	6.607	5.773	4.975	5.368	6.305	6.348
Ph-O-	-5.192	-0.864	6.609	5.775	4.977	5.383	6.320	6.363
Ph-CH_3	-5.187	-0.856	6.604	5.770	4.972	5.391	6.328	6.371
Kaolinite (001) face	-6.261	-5.267	7.678	6.844	6.046	0.980	1.917	1.960
Kaolinite (00-1) face	-6.260	-5.438	7.677	6.843	6.045	0.809	1.746	1.789
Octylphosphonic acid	-6.247	1.417						
Octylamine	-7.184	0.583						
Octanoic acid	-7.227	-0.215						

3.1.2. Adsorption energy, adsorption configuration, and electrostatic potential analysis

To validate the orbital analysis predictions and further assess adsorption stability, the adsorption configurations from Monte Carlo calculations were geometrically optimized, and the resulting adsorption energies were statistically compiled (Fig. 4). Octylphosphonic acid exhibits the lowest adsorption energy on kaolinite (00-1), confirming its most stable adsorption on this surface. Octylamine

shows the lowest energy on kaolinite (001), whereas octanoic acid yields relatively similar adsorption energies on kaolinite (001), (00-1), and the coal structural units, indicating little selectivity between kaolinite and coal surfaces.

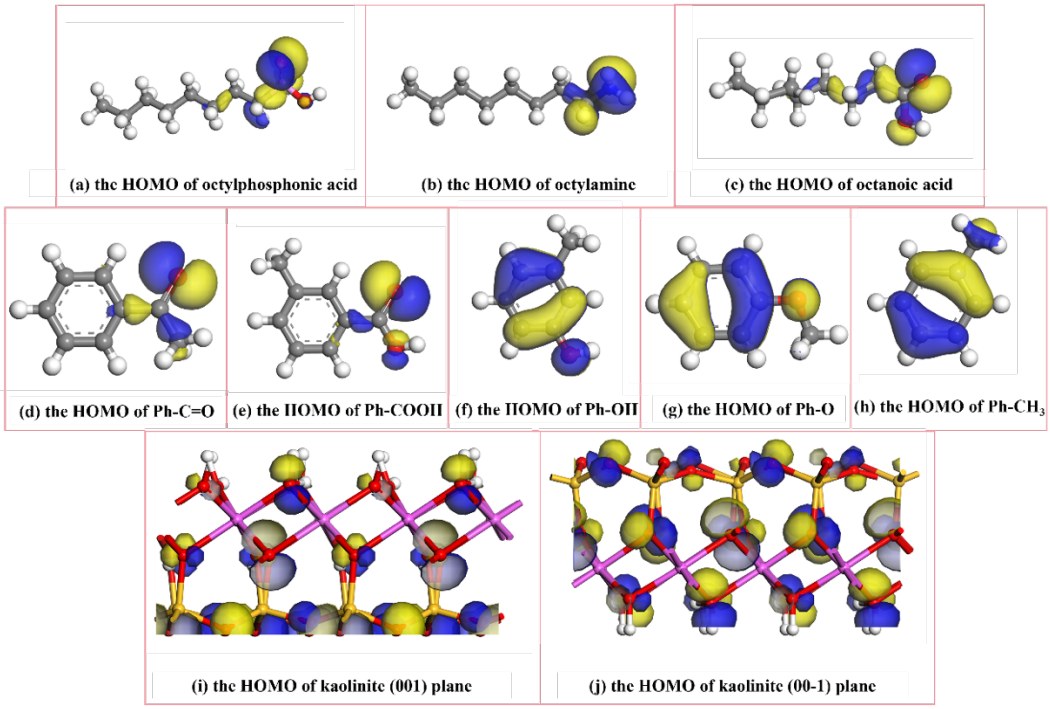


Fig. 3. Frontier orbitals of three reagents, kaolinite (001) face, kaolinite (00-1) face, and bituminous coal characteristic structural units

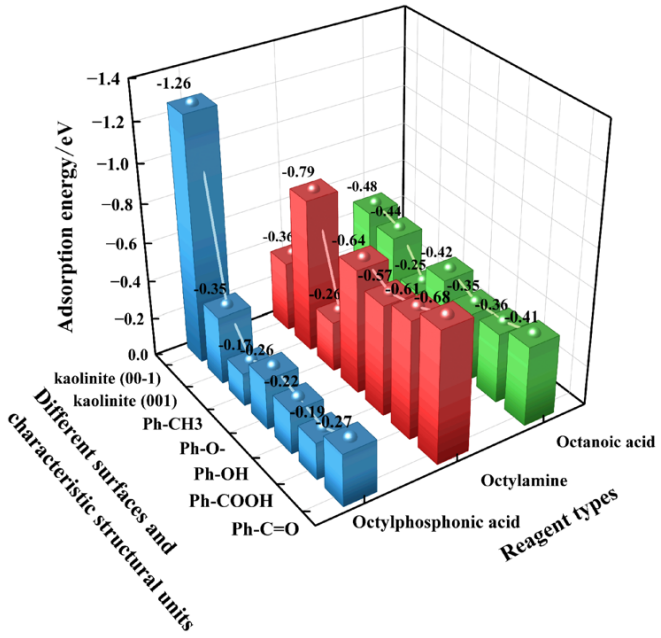
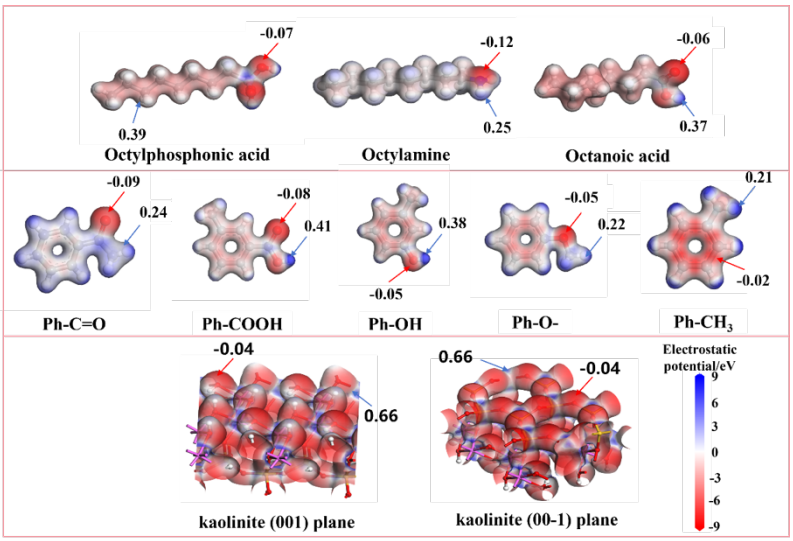
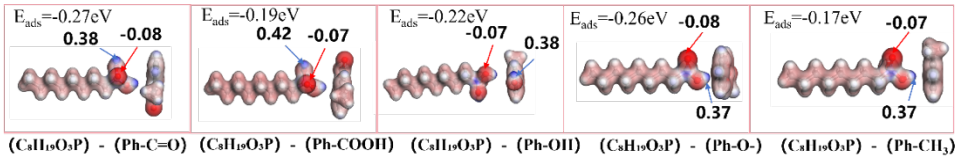


Fig. 4. Adsorption energies of three reagents on kaolinite (001) face, kaolinite (00-1) face, and bituminous coal characteristic structural units

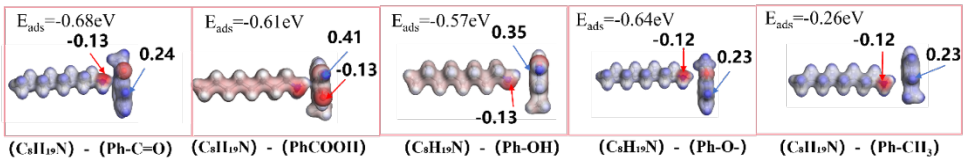
To further probe the adsorption mechanism, the electrostatic potential distributions of the optimized adsorption configurations were calculated (Fig. 5). In these distributions, negative-potential regions tend to donate electrons, indicating stronger nucleophilicity, whereas positive-potential regions tend to accept electrons, indicating stronger electrophilicity. As shown in Fig. 5(a), the negative electrostatic potential of the three reagents is primarily localized on their polar head groups. For the hydrophilic



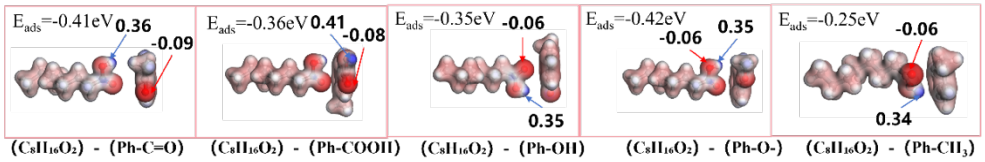
(a) Reagents, kaolinite surfaces, and bituminous coal characteristic structural units



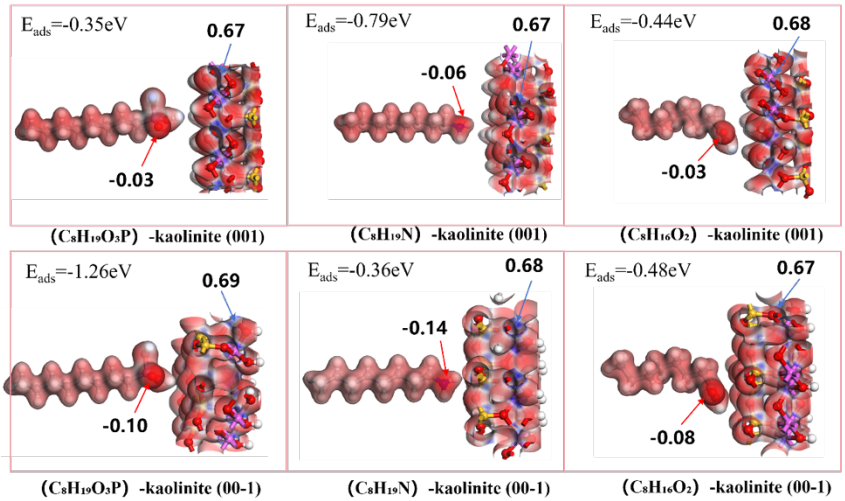
(b) Electrostatic potential distribution of octylphosphonic acid with bituminous coal characteristic structural unit



(c) Electrostatic potential distribution of octylamine with bituminous coal characteristic structural unit



(d) Electrostatic potential distribution of octanoic acid with bituminous coal characteristic structural unit



(e) Electrostatic potential distribution of reagents with kaolinite surfaces

Fig. 5. Adsorption configurations and electrostatic potential distributions of reagents with kaolinite surfaces and bituminous coal characteristic structural units (isosurface at 200 e/nm³)

structural units of bituminous coal, negative potential is mainly distributed on the oxygen-containing functional groups, while the highest positive potential appears on the H-atoms of these groups. Additionally, negative potential is also observed on the benzene rings. For both the kaolinite (001) and (00-1) surfaces, the isosurfaces exhibit negative potential throughout.

Fig. 5(b)–(d) show that octylphosphonic acid, octanoic acid, and octylamine adopt a perpendicular orientation relative to the hydrophilic structural units of bituminous coal. For octylphosphonic acid, the phosphonic head group contains both negative (=O) and positive (−OH) electrostatic potentials, providing electrostatic complementarity with the negatively charged kaolinite (00-1) surface. This complementarity underlies its lowest adsorption energy and most stable binding on that surface. In contrast, although the amino group of octylamine is positively charged, the negative potential on the kaolinite (00-1) surface is too weak to generate strong electrostatic attraction, resulting in its poor adsorption, consistent with the MD electrostatic energy data. On the coal surface, the positive potential of the oxygen-containing groups (−COOH, −C=O) on the bituminous coal structural units complements the negative potential of the octylamine head group, indicating an electrostatic mechanism for its strong adsorption on coal.

As shown in Fig. 5(e), octylphosphonic acid adopts a nearly perpendicular orientation on the kaolinite (00-1) surface, with its phosphonic head group directed toward the surface. The oxygen atoms of P＝O and P–OH exhibit close contact with the hydrogen atoms of the surface Al–OH groups, suggesting possible hydrogen bonding or coordination interactions. In contrast, in the configuration of octylamine on the kaolinite (00-1) surface, the amino group is located farther from the surface with a disordered orientation, corresponding to its weak interaction energy.

3.2. MD simulation results

To elucidate the atomic-scale interactions and adsorption selectivity of different functional groups, molecular dynamics (MD) simulations were performed for octylphosphonic acid, octanoic acid, and octylamine on kaolinite (001), (00-1), and coal surfaces. The adsorption behaviors were systematically compared in terms of interaction energies, self-diffusion coefficients, and relative concentration distributions, with molecular configurations also analyzed. The results provide a microscopic theoretical basis for understanding the intrinsic selectivity of the functional groups.

3.2.1. Interaction energy

The interaction energy between adsorbate and solid surface is a key indicator of adsorption spontaneity and strength. A negative value indicates a spontaneous process, and a larger absolute magnitude corresponds to stronger attraction and hence a more stable adsorption configuration (Ren et al., 2021). To elucidate the interaction behavior of the three functional groups on kaolinite (001), (00-1), and coal surfaces, the simulation-derived interaction energies were decomposed into total, electrostatic, and van der Waals components for detailed analysis. The detailed analysis is as follows:

$$E = \frac{1}{2}\left(E_t - E_{s-w} - E_{f-w} - E_s - E_f + E_{s-f} + E_w\right) \tag{12}$$

$$E_n = E_v + E_c \tag{13}$$

where E is the interaction energy, E_t is the total energy of the entire adsorption system, $E_{s\text{-}w}$,$E_{f\text{-}w}$, and $E_{s\text{-}f}$are the energies of the kaolinite (or coal) surface/water, reagent/water, and kaolinite (or coal) surface/reagent systems, respectively. E_s, E_f, and E_w are the energies of the kaolinite (or coal) surface, reagent molecule, and water molecule, respectively. E_n, E_v, and E_c are the non-bonding interaction energy, van der Waals energy, and Coulomb energy, respectively. In this study, the interaction energy mainly comes from non-bonding interactions, and all these energies are in kcal/mol.

As shown in Table 2, the absolute total interaction energies on the kaolinite (001) surface follow the order: octylamine (−134.68 kcal/mol) > octanoic acid (−93.09 kcal/mol) > octylphosphonic acid (−38.53 kcal/mol). Octylamine exhibits the largest total energy, with an electrostatic contribution (−71.51 kcal/mol) substantially exceeding those of octanoic acid (−36.18 kcal/mol) and octylphosphonic acid (−16.38 kcal/mol), indicating that the adsorption of amino-group on the (001) surface is primarily governed by electrostatic forces. In contrast, the van der Waals contributions also vary considerably among the three adsorbates. Octylamine and octanoic acid exhibit substantially larger van der Waals

interaction energies in magnitude than octylphosphonic acid, indicating that dispersion interactions also contribute to the differences in adsorption behavior. However, this baseline contribution is largely insensitive to the surface chemical environment and thus does not govern adsorption selectivity.

On the kaolinite (00-1) surface (Table 2), the absolute total interaction energies follow the order: octylphosphonic acid (−156.74 kcal/mol) > octanoic acid (−107.83 kcal/mol) > octylamine (−70.98 kcal/mol). Octylphosphonic acid exhibits the strongest adsorption affinity, with an electrostatic contribution of −109.37 kcal/mol, substantially higher than those of the other two reagents. This pronounced electrostatic interaction suggests that the phosphonic acid group likely engages in strong hydrogen bonding or coordination with the Al-OH surface. In marked contrast, octylamine shows the lowest total interaction energy (−70.98 kcal/mol) and a negligible electrostatic contribution of only −13.58 kcal/mol, indicating that its electrostatic attraction to the kaolinite (00-1) surface is extremely weak. This weak attraction may be attributed to the relatively low negative charge density of this surface.

On the coal surface (Table 2), the absolute total interaction energies follow the order: octylamine (−145.95 kcal/mol) > octanoic acid (−88.98 kcal/mol) > octylphosphonic acid (−40.22 kcal/mol). Octylamine exhibits the largest adsorption energy, with an electrostatic contribution of −82.82 kcal/mol, substantially exceeding those of octanoic acid (−33.19 kcal/mol) and octylphosphonic acid (−16.44 kcal/mol). This strong electrostatic interaction likely originates from the small number of oxygen- or nitrogen-containing functional groups present on the coal surface, which readily interact with the amino group. The van der Waals energies follow a similar trend: octylamine (−63.13 kcal/mol) > octanoic acid (−55.80 kcal/mol) > octylphosphonic acid (−23.78 kcal/mol), indicating that the hydrophobic alkyl chains also contribute to the overall adsorption affinity.

In summary, the three reagents show markedly different adsorption affinities toward the three surfaces. Octylphosphonic acid exhibits strong preferential adsorption on the kaolinite (00-1) surface but weak adsorption on the (001) and coal surfaces, indicating its selective recognition of the Al−OH surface. Octanoic acid shows moderate adsorption across all surfaces with no apparent selectivity. In contrast, octylamine adsorbs strongly on both kaolinite (001) and coal but weakly on (00-1), revealing its selectivity toward the siloxane surface and organic moieties.

Table 2. Interaction energies after adsorption of different reagents on different kaolinite faces and coal surface

Adsorption system	Adsorbate	Interaction energy (kcal/mol)	Electrostatic energy (kcal/mol)	van der Waals energy (kcal/mol)
Kaolinite (001) face	Octylphosphonic acid	-38.53	-16.38	-22.15
	Octanoic acid	-93.09	-36.18	-56.91
	Octylamine	-134.68	-71.51	-63.17
Kaolinite (00-1) face	Octylphosphonic acid	-156.74	-109.37	-47.37
	Octanoic acid	-107.83	-42.42	-65.41
	Octylamine	-70.98	-13.58	-57.39
Coal surface	Octylphosphonic acid	-40.22	-16.44	-23.78
	Octanoic acid	-88.98	-33.19	-55.80
	Octylamine	-145.95	-82.82	-63.13

3.2.2. Self-diffusion coefficient

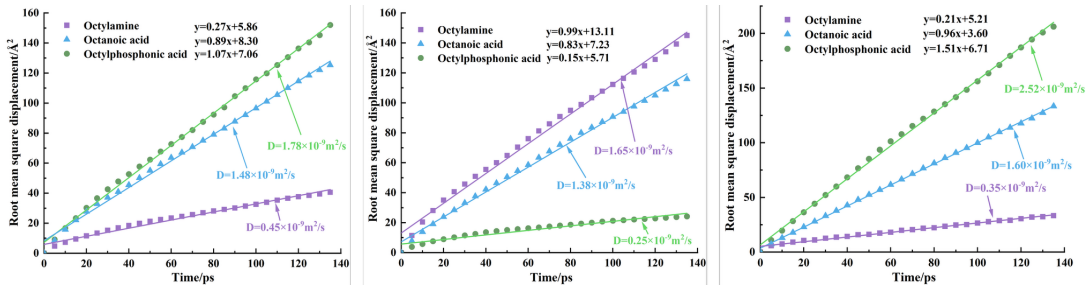
To probe the adsorption and diffusion behavior of the three reagents on kaolinite and coal, the mean square displacement (MSD) and self-diffusion coefficient (D) were derived from the MD trajectories (Fig. 6), with D defined as one-sixth of the slope obtained by linear fitting of the MSD curves (Wang et al., 2025).

On the kaolinite (001) surface (Fig. 6), the self-diffusion coefficients follow the order: octylphosphonic acid (1.78×10^{-9} m²/s) > octanoic acid (1.48×10^{-9} m²/s) > octylamine (0.45×10^{-9} m²/s). Octylamine exhibits the smallest diffusion coefficient, indicating its restricted mobility due to the strongest adsorption on this surface.

On the kaolinite (00-1) surface, the self-diffusion coefficients follow the order: octylamine (1.65×10^{-9} m²/s) > octanoic acid (1.38×10^{-9} m²/s) > octylphosphonic acid (0.25×10^{-9} m²/s). Compared with the (001) surface, the diffusion coefficient of octylphosphonic acid decreases dramatically, whereas that of octylamine increases notably, consistent with their respective adsorption strengths on this surface.

On the coal surface, the self-diffusion coefficients follow the order: octylphosphonic acid (2.52×10^{-9} m²/s) > octanoic acid (1.60×10^{-9} m²/s) > octylamine (0.35×10^{-9} m²/s). Octylamine shows the smallest value, while octylphosphonic acid exhibits the largest, correlating inversely with their adsorption affinities on the coal surface.

The above results reveal a negative correlation between the self-diffusion coefficient and adsorption strength on each surface: stronger adsorption (larger absolute interaction energy) corresponds to a smaller diffusion coefficient, whereas weaker adsorption permits higher molecular mobility. These findings confirm that the functional group type governs interfacial migration behavior by modulating the interaction energy.



(a) Kaolinite (001) (b) Kaolinite (00-1) (c) Coal surface

Fig. 6. Mean square displacement of different reagents after adsorption on kaolinite (001), (00-1) faces, and coal surface

3.2.3. Relative concentration distribution

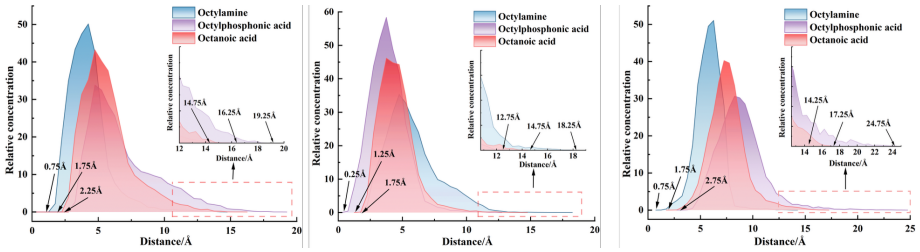
Relative concentration profiles, defined as the spatial distribution of adsorbates normal to the surface, characterize the adsorption layer structure and interfacial enrichment (Zhang et al., 2022). Fig. 7 presents these profiles for octylphosphonic acid, octanoic acid, and octylamine on the kaolinite (001), (00-1), and coal surfaces.

On the kaolinite (001) surface (Fig. 7a), octylamine exhibits the highest concentration peak closest to the surface, with a distribution range of 0.75–14.75 Å, narrower than those of octanoic acid (1.75–16.25 Å) and octylphosphonic acid (2.25–19.25 Å). This compact distribution near the surface reflects the strongest interfacial enrichment of octylamine on this surface.

On the kaolinite (00-1) surface (Fig. 7b), octylphosphonic acid shows the highest concentration peak nearest to the surface, with a distribution range of 0.25–12.75 Å, substantially narrower than those of octanoic acid (1.25–14.75 Å) and octylamine (1.75–18.25 Å). The smallest starting distance and narrowest range indicate the strongest surface localization of octylphosphonic acid on this surface.

On the coal surface (Fig. 7c), octylamine presents the highest concentration peak closest to the surface, with a distribution range of 0.75–14.25 Å, narrower than those of octanoic acid (1.75–17.25 Å) and octylphosphonic acid (2.75–24.75 Å). In contrast, octylphosphonic acid shows the broadest distribution, suggesting its weakest surface confinement on the coal surface.

The above results reveal a consistent correlation among relative concentration profiles, adsorption strengths, and diffusion coefficients. Specifically, stronger adsorption (larger absolute interaction energy) yields a higher, sharper concentration peak located closer to the surface, whereas weaker adsorption produces a lower and more dispersed peak. This relationship is exemplified by octylamine on kaolinite (001) and coal, and by octylphosphonic acid on kaolinite (00-1), all of which exhibit the highest, nearest, and narrowest concentration peaks, consistent with their strongest adsorption and lowest diffusion. Overall, the functional group type governs the adsorption configuration, mobility, and spatial distribution of adsorbates by modulating the interfacial interaction strength; stronger adsorption corresponds to tighter confinement near the surface.



(a) Kaolinite (001) (b) Kaolinite (00-1) (c) Coal surface

Fig. 7. Relative concentration of different reagents after adsorption on kaolinite (001), (00-1) faces, and coal surface

3.3. Flotation test verification

To further validate the predicted selectivity of the three functional groups from DFT calculations and MD simulations, flotation experiments were performed to assess their macroscopic separation performance. In this section, macroscopic flotation separation selectivity is defined as the ability to preferentially recover kaolinite while minimizing coal reporting to the concentrate. This is distinct from the intrinsic surface-recognition selectivity evaluated by DFT and MD simulations. A reagent with high selectivity for kaolinite flotation should preferentially float kaolinite while minimizing coal recovery.

Fig. 8 presents the flotation results for octylphosphonic acid, octanoic acid, and octylamine at varying dosages. The concentrate yield (mass percentage of froth product in the total feed) reflects the overall collecting ability of the reagent toward both coal and kaolinite. As shown in Fig. 8(a), octylphosphonic acid causes a sharp yield increase from 25.56% to 39.72% at 150 g/t, then gradually rises and plateaus, indicating strong overall collecting ability toward both coal and kaolinite. Octanoic acid reaches its maximum yield of 50.69% at 300 g/t, followed by a slight decline upon overdosing, demonstrating the strongest collecting capacity but with inhibition at high dosage. Octylamine exhibits a peak yield of 46.25% at 450 g/t after an initial rise and a subsequent small drop, reflecting relatively weak overall collecting ability.

Concentrate ash content reflects the proportion of kaolinite in the froth product, serving as a key quality indicator: higher ash values indicate greater kaolinite enrichment in the concentrate. As shown in Fig. 8(b), octylphosphonic acid induces a sharp ash increase to 78.37% (near pure kaolinite ash). Although the ash declines slightly thereafter, it remains consistently high, confirming strong kaolinite collection. In contrast, octanoic acid produces a sharp jump to 54.11% at 300 g/t and continues to rise thereafter, revealing a clear dosage threshold. Meanwhile, octylamine reduces the ash to 22.89%–26.13% at low dosages (below the blank level) and reaches the blank level at 450 g/t. This value is substantially lower than those of the other two reagents, indicating very weak kaolinite adsorption and a certain depression effect.

Combustible recovery represents the proportion of coal (combustible matter) reporting to the concentrate. In this study, the target is kaolinite flotation; therefore, a lower combustible recovery is desirable because it indicates stronger suppression of coal and favors kaolinite enrichment in the concentrate. As shown in Fig. 8(c), octylphosphonic acid sharply reduces the recovery from 39.92% to 18.51% and maintains it below 30%, strongly suppressing coal flotation and thus favoring kaolinite enrichment in the concentrate. Octanoic acid reaches a peak recovery of 60.64% at 150 g/t, followed by a continuous decline, exhibiting coal suppression only at high dosage. In contrast, octylamine achieves a maximum recovery of 72.98% at 450 g/t and remains above 61% over a broad dosage range, demonstrating the best coal recovery, which is unfavorable for kaolinite flotation.

Kaolinite recovery, defined as the proportion of kaolinite reporting to the concentrate, serves as the most direct indicator of reagent adsorption and collection on kaolinite. As shown in Fig. 8(d), octylphosphonic acid exhibits the highest kaolinite recovery of 60.93% at 150 g/t and remains consistently high, demonstrating very strong collecting ability toward kaolinite and making it the most promising reagent for kaolinite flotation. Octanoic acid shows a sharp increase from 21.03% to 50.64% at 300 g/t, suggesting a clear threshold effect, with intermediate performance. By contrast, octylamine reaches only 25.93% at 600 g/t, substantially lower than those of the other two reagents, indicating extremely weak kaolinite collection; it therefore preferentially floats coal rather than kaolinite and is unsuitable for kaolinite flotation.

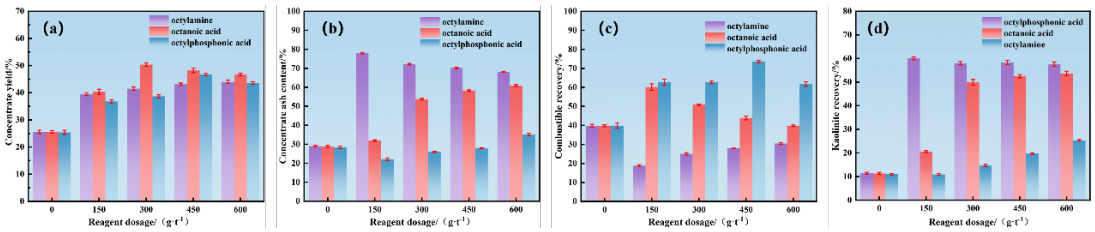


Fig. 8. Flotation results at different reagent dosages: (a) Concentrate yield; (b) Concentrate ash; (c) Combustible recovery; (d) Kaolinite recovery

3.4. Multiscale consistency among MD, DFT, and flotation results

The MD and DFT results were obtained at different scales and with different energy references: MD interaction energies are expressed in kcal/mol and include the total non-bonded contribution of the adsorption system, whereas DFT adsorption energies are expressed in eV and describe the electronic binding of a single molecule on a characteristic surface unit. Their absolute values should therefore not be compared directly. Nevertheless, their trends are highly consistent and mutually reinforcing.

On the coal surface, MD gives the absolute interaction energy order: octylamine (-145.95 kcal/mol) > octanoic acid (-88.98 kcal/mol) > octylphosphonic acid (-40.22 kcal/mol). The DFT adsorption energies on the bituminous coal structural units follow the same order: octylamine (-0.57 to -0.68 eV) > octanoic acid (-0.35 to -0.42 eV) > octylphosphonic acid (-0.17 to -0.27 eV). Thus, both methods independently indicate that octylamine exhibits the strongest adsorption on coal.

On kaolinite (00-1) surface, MD gives octylphosphonic acid (-156.74 kcal/mol) > octanoic acid (-107.83 kcal/mol) > octylamine (-70.98 kcal/mol), while DFT gives octylphosphonic acid (-1.26 eV) > octanoic acid (-0.48 eV) > octylamine (-0.36 eV). Both methods therefore converge in identifying octylphosphonic acid as the most strongly adsorbed molecule on the target Al-OH surface.

On kaolinite (001) surface, both MD and DFT again agree that octylamine exhibits the strongest adsorption, followed by octanoic acid, with octylphosphonic acid the weakest. The three methods thus form a consistent chain: MD describes the interfacial adsorption strength and molecular mobility, DFT identifies the electronic origin of the head-group–surface interaction, and flotation reflects the macroscopic separation outcome.

This consistency is further confirmed by the flotation results. When the target is kaolinite flotation, octylphosphonic acid gives the highest kaolinite recovery (60.93%) and concentrate ash (78.37%) while maintaining a low combustible recovery, consistent with its strong adsorption on kaolinite (00-1) and weak adsorption on coal. Octylamine gives the highest combustible recovery (72.98%) and the lowest kaolinite recovery (<26%), consistent with its strong adsorption on coal and kaolinite (001) and weak adsorption on kaolinite (00-1). Octanoic acid is intermediate in both simulation and flotation. Taken together, the MD, DFT, and flotation results are not merely coexistent but mutually corroborating, jointly supporting the conclusion that the phosphonic acid group is the preferred head group for kaolinite flotation, whereas the amino group preferentially floats coal and is therefore unsuitable for kaolinite flotation.

The initial pulp pH ranged from 6 to 8, and no deliberate pH adjustment was performed. The ionization states of the phosphonic acid, carboxyl, and amino groups may vary with pH, while the surface charge characteristics of kaolinite may also be affected by the solution pH. These factors may influence the interfacial interactions between the reagents and the solid surfaces and, consequently, the observed flotation selectivity. Therefore, the flotation results should be interpreted within the recorded initial pulp pH range, and the possible influence of pH should be considered when comparing the flotation performance of the three reagents. Because pH was not systematically controlled, its individual contribution to the observed flotation differences cannot be isolated from the present experiments.

4. Conclusions

This study integrates density functional theory (DFT) calculations, molecular dynamics (MD) simulations, and flotation experiments to systematically elucidate the differential interaction behavior of three representative reagents (octylphosphonic acid, octanoic acid, and octylamine) on kaolinite (001),

(00-1), and coal surfaces, spanning electronic interactions, microscopic adsorption, and macroscopic separation performance. The main conclusions are as follows:

(1) DFT calculations show that octylphosphonic acid has the smallest orbital energy gap with kaolinite (00−1) (0.809 eV) and optimal electrostatic complementarity with the Al−OH surface, confirming the electronic origin of its selective adsorption.

(2) MD simulations reveal that octylphosphonic acid exhibits the strongest adsorption on kaolinite (00−1) (−156.74 kcal/mol), with the lowest diffusion (0.25×10^{-9} m²/s) and the narrowest interfacial distribution (0.25–12.75 Å), indicating high selectivity for the Al−OH surface and strong surface confinement, which is favorable for kaolinite flotation. Octylamine adsorbs strongly on both kaolinite (001) (−134.68 kcal/mol) and coal (−145.95 kcal/mol), but weakly on kaolinite (00-1), indicating that it preferentially interacts with coal and the siloxane surface rather than the target Al-OH surface and is therefore unsuitable for kaolinite flotation. Octanoic acid shows intermediate adsorption on all surfaces.

(3) Flotation tests validate the simulation predictions when kaolinite flotation is the target. Octylphosphonic acid gives the highest kaolinite recovery (60.93%) and concentrate ash (78.37%) while strongly suppressing combustible recovery, confirming its strong affinity for kaolinite and making it the most promising reagent for kaolinite flotation. Octylamine gives the highest combustible recovery (72.98%) and the lowest kaolinite recovery (<26%), indicating that it preferentially floats coal and suppresses kaolinite and is therefore unsuitable for kaolinite flotation. Octanoic acid exhibits intermediate performance.

(4) For kaolinite flotation, the phosphonic acid group, with specific recognition for the kaolinite (00-1) Al-OH surface, is suitable for constructing selective collectors or flocculants for kaolinite. The amino group, despite strong coal affinity, preferentially floats coal and lacks sufficient selectivity for kaolinite and should not be used alone for kaolinite flotation. The carboxyl group serves as a moderate modulator. This study provides a theoretical foundation for the molecular design of reagents for kaolinite flotation.

Acknowledgements

This work was supported by the National Nature Science Foundation of China (Grant nos. 52274251, 52604414), the Scientific Research Foundation for High-level Talents of Anhui University of Science and Technology(2024yjrc68), and the Analytical and testing center of University of Science and Technology.

References

ARCOS F., JIMENEZ G., URIBE L., et al., 2026, *The effect of anionic polyacrylamides in process water on chalcopyrite flotation in the presence of kaolinite*. Miner. Eng., 237, 110020.

CHEN J., CHU X., GE W., et al., 2022, *Synergetic adsorption of dodecane and dodecylamine on oxidized coal: Insights from molecular dynamics simulation*. Appl. Surf. Sci., 592, 153103.

CHEN J., MIN F., LIU L., et al., 2020, *Systematic exploration of the interactions between Fe-doped kaolinite and coal based on DFT calculations*. Fuel, 266, 117082.

CHENG Y., CHEN J., MIN F., et al., 2023, *Research on the flotation efficiency of alcohol/ether alcohol frothers for common collectors: Insight of molecular dynamics simulations*. Appl. Surf. Sci., 614, 156233.

CLARK S.J., SEGALL M.D., PICKARD C.J., et al., 2005, *First principles methods using CASTEP*. Zeitschrift für Kristallographie – Crystalline Materials, 220(5–6), 567–570.

DEY S., PATRA A.S., PATRA P., et al., 2022, *Macromolecular selective flocculant derived from functionalized starch towards beneficiation of low-quality iron ore: Atomistic simulations and experimental studies*. Mater. Today Commun., 32, 103810.

HUANG T., LI Z., XIE P., et al., 2026, *Regulation of lignin functional groups and adsorption mechanism on the surface of a-FeOOH*. Appl. Surf. Sci., 720, 165196.

KHALIL R.M.A., HUSSAIN F., HUSSAIN M.I., et al., 2020, *The investigation of optoelectronic, magnetic and dynamical properties of Ce and Ti doped 2D blue phosphorene: A dispersion corrected DFT study*. J. Alloys. Compd., 827, 154255.

LIU L., MIN F., CHEN J., et al., 2019, *The adsorption of dodecylamine and oleic acid on kaolinite surfaces: Insights from DFT calculation and experimental investigation*. Appl. Surf. Sci., 470, 27–35.

LU Q., ZHANG F., HUANG H., et al., 2026, *Influence of aluminum species distribution in polyaluminum chloride on the mitigation of fine kaolinite entrainment in coal flotation*. Miner. Eng., 245, 110343.

LV J., ZHANG C., LI J., et al., 2026, *Selective flocculation mechanism of sodium oleate in flotation separation of cassiterite and calcite with cetylpyridinium bromide as a dispersant*. Miner. Eng., 238, 110079.

NG W.S., CONNAL L.A., FORBES E., et al., 2016, *Xanthate-functional temperature-responsive polymers as selective flocculants and collectors for fines recovery*. Miner. Eng., 96–97, 73–82.

NG W.S., THOMAS C.A., FORBES E., et al., 2026, *Identifying opportunities for the selective flocculation-flotation of fine valuable minerals: A techno-economic analysis*. Miner. Eng., 235, 109884.

NIU F., CHEN Y., ZHANG J., et al., 2024, *Selective flocculation-flotation of ultrafine hematite from clay minerals under asynchronous flocculation regulation*. Int. J. Min. Sci. Technol., 34, 1563–1574.

PENG W., LV S., CAO Y., et al., 2023, *A novel pH-responsive flocculant for efficient separation and recovery of Cu and Mo from secondary resources via selective flocculation-flotation*. J. Clean. Prod., 395, 136463.

PERDEW J.P., BURKE K., ERNZERHOF M., 1996, *Generalized Gradient Approximation Made Simple*. Phys. Rev. Lett., 77(18), 3865–3868.

REN B., LV K., MIN F., et al., 2021, *A new insight into the adsorption behavior of NPAM on kaolinite/water interface: Experimental and theoretical approach*. Fuel, 303, 121299.

SEGALL M.D., LINDAN P.J.D., PROBERT M.J., et al., 2002, *First-principles simulation: ideas, illustrations and the CASTEP code*. J. Phys. Condens. Matter, 14, 2717.

SHI P., WANG S., MA F., et al., 2026, *Effect of grafted groups on adsorption conformation and adsorption behavior of guar gum: insights from molecular interactions*. Carbohydr. Polym., 378, 124974.

WANG L., MIN F., SUN K., et al., 2025, *Exploration of interaction between different types of flocculants and coal particles based on experiments and simulations*. Surf. Interfaces, 59, 105903.

WANG Y., ZHOU W., LI Y., et al., 2021, *The role of polyvinylpyrrolidone in the selective separation of coal from quartz and kaolinite minerals*. Colloids Surf. Physicochem. Eng. Asp., 626, 126948.

XIA W., LI Y., WU F., et al., 2021, *Enhanced flotation selectivity of fine coal from kaolinite by anionic polyacrylamide pre-conditioning*. J. Mol. Liq., 334, 116083.

XIA Y., ZHANG S., TANG X., et al., 2024, *Selective adsorption of methylene blue dye by a flocculation sludge-derived adsorbent prepared by carboxymethyl chitosan-based flocculants*. Int. J. Biol. Macromol., 278, 134997.

YANG Z., XIA Y., FU Y., et al., 2025, *The flotation deashing separation performance of high-ash fine coal-slime using humic acid depressant and insights to its depressant mechanism*. Fuel, 382, 133756.

YUAN J., LU H., GONG X., et al., 2026, *Effects of high-efficiency depressant carboxymethyl chitosan on the flotation separation of fine-grained ilmenite and titanaugite: Experimental investigation and mechanism analysis*. Appl. Surf. Sci., 718, 164881.

ZHANG D., LI Y., HUANG Y., et al., 2022, *Interaction between PAM and kaolinite (0 0 1) surface in aqueous solution, insights from DFT and MD simulations*. Appl. Surf. Sci., 604, 154576.

ZHANG J., YANG C., NIU F., et al., 2022, *Molecular dynamics study on selective flotation of hematite with sodium oleate collector and starch-acrylamide flocculant*. Appl. Surf. Sci., 592, 153208.

ZHANG L., MIN F., CHEN J., et al., 2022, *New insights into the interaction between monomers from acrylamide-based polymeric flocculants and montmorillonite: A DFT study*. J. Mol. Liq., 365, 120171.

ZHANG S., MA H., GAO N., et al., 2025, *Enhanced flocculation performance and coal slurry water by using starch-based flocculant with rich charges and its flocculation mechanism*. J. Environ. Manage., 381, 125112.

ZHANG Y., LI S., MA X., et al., 2026, *Research progress on selective flocculation-flotation of fine-grained hematite*. Miner. Eng., 247, 110448.

ZOU W., GONG L., HUANG J., et al., 2019, *Adsorption of hydrophobically modified polyacrylamide P(AM-NaAA-C16DMAAC) on model coal and clay surfaces and the effect on selective flocculation of fine coal*. Miner. Eng., 142, 105887.